AIP | Review of Scientific Instruments

Note: Three-dimensional stereolithography for millimeter wave and terahertz applications

A. Macor, E. de Rijk, S. Alberti, T. Goodman, and J-Ph. Ansermet

Citation: Rev. Sci. Instrum. **83**, 046103 (2012); doi: 10.1063/1.3701738
View online: http://dx.doi.org/10.1063/1.3701738
View Table of Contents: http://rsi.aip.org/resource/1/RSINAK/v83/i4
Published by the American Institute of Physics.

Related Articles

Statistically modified surfaces: Experimental solutions for controlled scattered light
J. Appl. Phys. 112, 114325 (2012)

Design and optimization of a light-emitting diode projection micro-stereolithography three-dimensional manufacturing system
Rev. Sci. Instrum. 83, 125001 (2012)

An optical leveling technique for parallel near-field photolithography system
Appl. Phys. Lett. 101, 173112 (2012)

High-speed plasmonic nanolithography with a solid immersion lens-based plasmonic optical head
Appl. Phys. Lett. 101, 161109 (2012)

Hybrid organic/GaN photonic crystal light-emitting diode
Appl. Phys. Lett. 101, 141122 (2012)

Additional information on Rev. Sci. Instrum.

Journal Homepage: http://rsi.aip.org
Journal Information: http://rsi.aip.org/about/about_the_journal
Top downloads: http://rsi.aip.org/features/most_downloaded
Information for Authors: http://rsi.aip.org/authors

ADVERTISEMENT

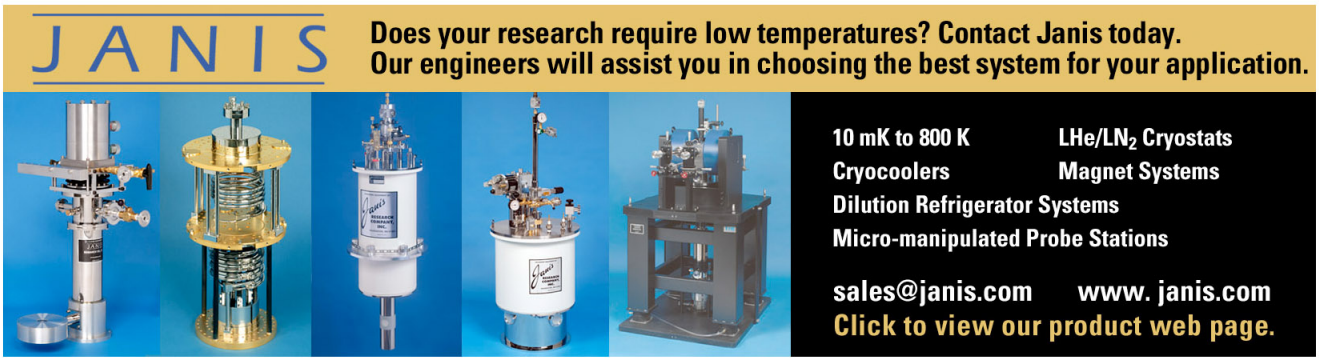

Note: Three-dimensional stereolithography for millimeter wave and terahertz applications

A. Macor,[1,2] E. de Rijk,[1,2,a)] S. Alberti,[3] T. Goodman,[3] and J-Ph. Ansermet[1]
[1]*Institute of Condensed Matter Physics, Station 3, EPFL, 1015 Lausanne, Switzerland*
[2]*SWISSto12 Sàrl, 1015 Lausanne, Switzerland*
[3]*Centre de Recherche en Physique des Plasmas, Station 13, EPFL, 1015 Lausanne, Switzerland*

(Received 6 January 2012; accepted 20 March 2012; published online 6 April 2012)

Metal-coated polymers shaped by 3D stereolithography are introduced as a new manufacturing method for passive components for millimeter to terahertz electromagnetic waves. This concept offers increased design capabilities and flexibilities while shortening the manufacturing process of complex shapes, e.g., corrugated horns, mirrors, etc. Tests at 92.5, 140, and 170 GHz are reported. © *2012 American Institute of Physics*. [http://dx.doi.org/10.1063/1.3701738]

Passive components are used to propagate or manipulate electromagnetic waves. Typical examples in the millimeter to terahertz frequency range are waveguides, horn antennas, tapers, mirrors, miter bends, directional couplers, diffraction structures, etc. Reflective metallic surfaces of components are smooth or corrugated. In the latter case, corrugations act as diffraction structures with dimensions that scale with the electromagnetic wavelength. When working at frequencies reaching the upper limit of the millimeter wave range, at 300 GHz or higher, the manufacturing of passive components becomes challenging and often costly when relying on techniques such as conventional machining and/or electro-forming. The latter technique being limited by its complex procedures while conventional machining can no longer be employed when physical dimensions of the components get small compared to machining tools such as chasers.[1] The upper limit of the millimeter wave range, merging with the terahertz frequency range, is a frontier area for research in physics,[2] astrophysics,[3] plasma physics,[4] chemistry,[5] material science,[6] biology,[7] and medicine.[8] This growing interest motivates a strong effort to develop the necessary technology to implement new experiments, techniques, and applications.

In this note, we introduce metal-coated polymers shaped by 3D stereolithography as a new construction method for passive components for millimeter to terahertz electromagnetic waves (patent pending).

Compared to previous work,[9] the employed technique allows the coating of closed complex surfaces such as in corrugated antennas, ortho-mode transducers, etc.

By using 3D stereolithography, computer-aided drawings can be converted directly into solid 3D objects without intermediate steps.[10] These objects are created in polymeric non-conductive materials. The surfaces requiring the reflection and scattering of the electromagnetic signals have therefore to be metal-coated in a second step.[11] Nowadays, the accuracy of stereolithography techniques can reach nanometric scales in small volumes of few cubic micrometers.[12] By reducing the manufacturing accuracy, microwave and the terahertz wave components occupying volumes on the order of 10 dm^3 can be manufactured using commercially available 3D printers. With these, the accuracy of 3D stereolithography can be roughly estimated taking into account the fluctuations of the laser beam profile used in the manufacturing process. The accuracy of the process in three dimensions (XYZ) for objects with dimensions of several centimeters is of the order of ± 20 μm in the XY-plane and ± 50 μm in the Z-direction.[10]

This manufacturing accuracy is sufficient to obtain a large variety of passive components for millimeter, submillimeter, and possibly terahertz waves applications. In this note, the plastic objects obtained by 3D stereolithography are metal coated by using an electroless plating (ELP) technique.[13] This metallization technique has become increasingly attractive because of its simplicity and low cost. ELP is a chemical process employed for the metallization of non-conductive substrates, such as plastics, glasses, and ceramics, without the use of external fields. First, the non-conductive surfaces are activated by a deposition of cationic metallic ions, thereafter the activated surfaces are coated in a solution containing a gold salt. Typical deposition rates for the gold coating process amount to a few hundreds of nanometers per hour, which made it possible to reach gold coating thicknesses on the order of 1 μm. For a conductive layer to be highly reflective, it has to have a thickness over at least three times the skin depth, Eq. (1), at that particular frequency γ. With the magnetic permeability and the resistivity of gold: $\mu_{gold} \approx (1 + 10^{-6})\mu_0$, $\rho_{gold} = 2.44 \times 10^{-8}\ \frac{\Omega}{m}$, we see that the golden coating thickness necessary for components operating above 50 GHz is smaller than 1 μm,

$$\delta = \sqrt{\frac{\rho}{\pi \gamma \mu}}. \tag{1}$$

To test the robustness of this manufacturing technique, several passive components have been built using this 3D stereolithography. The following paragraphs expose these components and their characteristics.

Figure 1(a) shows two polarizers manufactured as corrugated mirrors with the same geometrical proprieties and designed to control the electric field orientation of a linearly polarized beam at 140 GHz upon reflection on the mirror as explained in detail by Felici *et al.*[14] One mirror

a)Electronic mail: emile.derijk@epfl.ch.

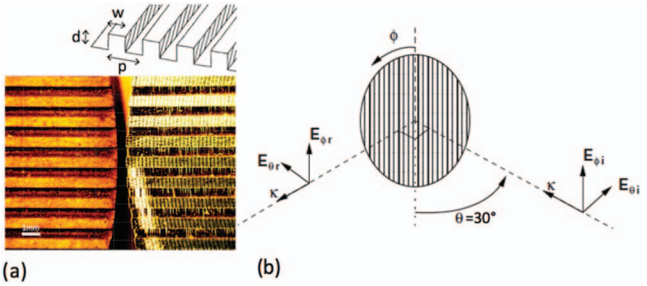

FIG. 1. (a) Bottom left: corrugated metal-coated plastic mirror. Bottom right: corrugated aluminum mirror. Top: corrugation characteristics for both mirrors: $p = 0.53$ mm, $d = 0.265$ mm, and $w = 0.28$ mm. (b) Experimental setup, with the linear polarization electric field components for both the incident and reflected beams at 140 GHz. The incidence angle is of 30° with the incident beam being linearly polarized in the vertical direction, i.e., $E_{\theta i} = 0$. $E_{\theta r}$ and $E_{\phi r}$ are independently measured as a function of ϕ by using a fundamental TE_{10} rectangular waveguide antenna mounted on a Schottky diode detector.

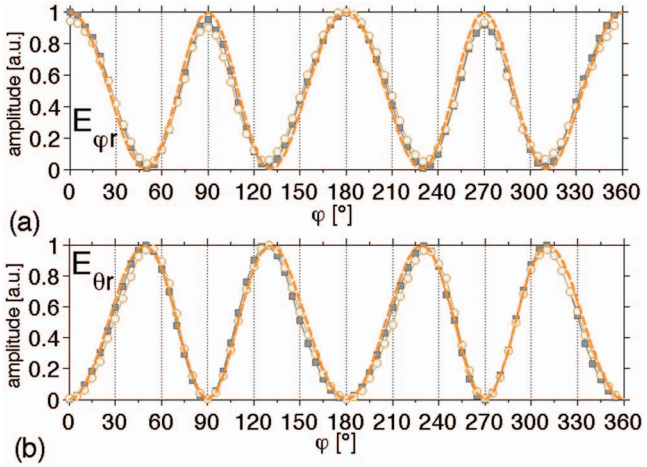

FIG. 2. Normalized signal amplitude of the beam reflected on the mirror versus rotation angle of the mirror's linear corrugations. (a) TE_{10} waveguide oriented to measure field components parallel to the linear polarization incident on the mirror. (b) TE_{10} waveguide oriented to measure field components perpendicular to the linear polarization incident on the mirror. Dashed lines: simulated data. Squares: measurements using the conventional machined aluminum polarizer. Circles: measurements using the metal-coated plastic polarizer. Error on measurements on the order of 0.01%.

is a conventionally machined in aluminum, the other one being a metal-coated plastic mirror. In the experiments, a linearly polarized Gaussian beam at 140 GHz is shined upon the flat corrugated mirror with an incidence angle of 30°. The mirror can be rotated, without changing the incidence angle of beam, while the angle between the incident beam's linear polarization and the mirror's corrugations is changed. This rotation is used to modify the interference conditions upon reflection on the mirror and control the orientation of the linear polarization of the beam, Fig. 1(b). The reflected beam is measured by using a fundamental TE_{10} rectangular waveguide antenna mounted on a Schottky diode detector, collecting a small portion of the reflected fields. The Schottky diode output dc voltage is proportional to the field intensity associated with the electric field component determined by the orientation of the fundamental TE_{10} waveguide.

Figure 2 shows this experimental characterization of the beam reflected by the polarizers. Relative maxima in the measured beam intensity, panel 2(a), indicate the orientations of the mirror's corrugations for which the incoming linear polarization orientation is preserved after reflection, resp., relative minima indicate that the incident linear polarization orientation rotated by 90° after reflection. On panel 2(b), the same measurement is reported when the TE_{10} waveguide used for detection is rotated by 90°, thus measuring the intensities of the orthogonal polarization. The behavior of the mirrors built by metal-coated plastics is shown to be quasi-identical to that of the conventional machined aluminum mirrors. The data conform very well with the results of electromagnetic simulations.[15]

As a second validation of this manufacturing concept, we manufactured a 15 cm diameter quadratic phase correction mirror for electron cyclotron resonance heating plasma heating applications. This mirror has an astigmatic spherical shape. It is used to modify the profile of an incident free space propagating beam upon reflection. For the experiments presented here, the incident beam at 170 GHz is launched from a Gaussian optics lens antenna (GOLA) attached to a standard, 63.5 mm diameter, corrugated aluminum waveguide. The beam has an incidence angle of 10° upon the phase correction mirror. The beam spot size (transverse to its propagation) after reflection is measured experimentally using a Schottky diode detector mounted on a robot for systematic spacial sampling. The experimental results are compared to the theoretical predictions in Fig. 3. Theoretical predictions are based on an ideal HE_{11} mode generated at the output of the GOLA antenna which is numerically propagated[16] and reflected onto the phase correction mirror.

As a further test of the flexibility of the technique, a smooth wall horn antenna for an electron cyclotron diagnostic system at 92.5 GHz is presented. The horn is specifically designed to reduce side lobes of the beam it radiates while increasing its directionality. The internal shape of the horn antenna[17] is given by Eq. (2), for the radius, $a(z)$, along the

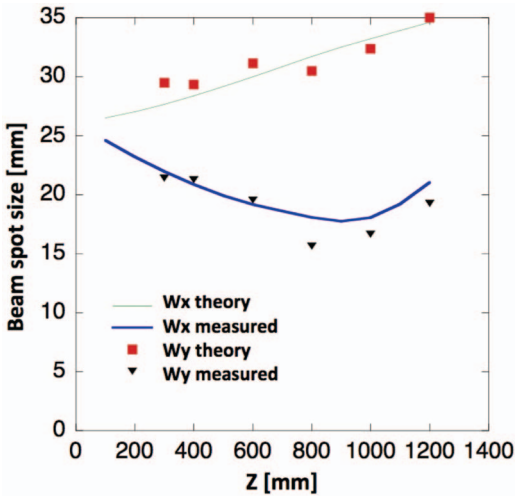

FIG. 3. Measured (dots) and simulated (solid line), beam spot size after reflection of a TEM_{00} Gaussian beam upon the quadratic phase correction mirror. The propagation of the reflected wave is along the Z direction, the beam spot sizes are plotted for the X and Y directions.

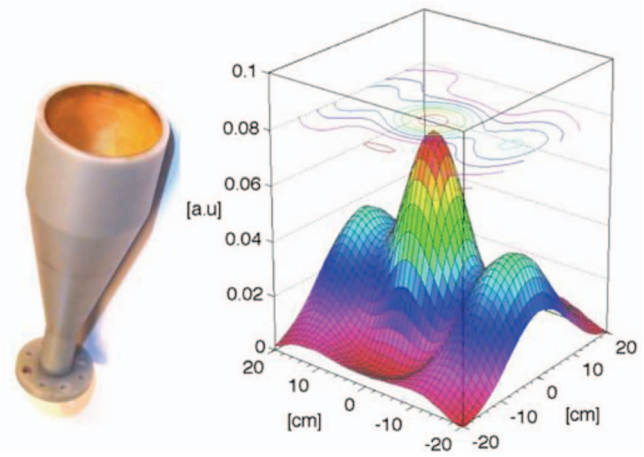

FIG. 4. Left, metal-coated plastic smooth wall horn antenna for signal modulation at 92.5 GHz. Measured beam intensity on a cross section at 10 cm of the horn's large aperture output.

horn axis z,

$$a(z) = \begin{cases} f(z)) & z < L/2 \\ -f(L-z) + 2f(L/2)) & z \geq L/2 \end{cases}, \quad (2)$$

$$f(z) = a_1 \sqrt{1 + \left(\frac{z}{\alpha\, k\, a_1}\right)^2}. \quad (3)$$

α is a parameter that controls the slope, k the wavenumber, $L = 48$ mm the total horn length, and $a_1 = 1, 6$ mm the the cut-off radius.

A picture of the horn is shown in Fig. 4(left). A beam intensity measurement on a cross section of the beam 10 cm from the horn's exit is shown in Fig. 4(right). A detailed analysis of the experimental data and comparison to simulations is underway in order to validate the horn design.

In addition to mirrors and antennas, for millimeter to THz waves, corrugated HE_{11} transmission lines must be used in order to propagate signals with the highest fidelity and lowest losses. In a previous work, we demonstrated the possibility of forming this corrugation by stacking rings.[18] As a perspective, tests are ongoing to realize such corrugations by 3D stereolithography.

The technique described in this note shows the ability to build entirely modular transmission lines using 3D stereolithography in conjunction with a surface metal coating. In summary, the examples shown in this note validate the idea of using 3D stereolithography with electroless plating to make components for millimeter waves and THz technology, opening the way to a cost-effective production with unprecedented design flexibility and short manufacturing times.

The authors thank all the EPFL staff involved: G. Grandjean and O. Haldimann at the IPMC, R. Bertizzolo and S. Allenspach at CRPP, F. Felici for the simulations of Fig. 2, L. Porte and F. Li, who tested the horn design of Fig. 4, and M. Abid for his essential support. Work supported by Requip (206021-121303/1), Sinergia (CRSI20-122708/1), and (200020-120503/1) grants of the Swiss National Science Foundation and by the EPFL.

[1]P. Woskov, E. Nanni, M. Shapiro, S. Jawla, J. Hummelt, R. Temkin, and A. Barnes, in *36th International Conference on Infrared Millimeter and Terahertz Waves (IRMMW-THz)* (2011).
[2]B. E. Cole, J. B. Williams, B. T. King, M. S. Sherwin and C. R. Stanley, Nature (London) **410**, 60–63 (2001).
[3]G. L. Pilbratt, J. R. Riedinger, T. Passvogel, G. Crone, D. Doyle, U. Gageur, A. M. Heras, C. Jewell, L. Metcalfe, S. Ott, and M. Schmidt, Astron. Astrophys. **518**, L1 (2010).
[4]J. L. Doane, Fusion Sci. Technol. **53**, 159–173 (2008).
[5]R. G. Griffin and T. F. Prisner, Phys. Chem. Chem. Phys. **12**, 5737–5740 (2010).
[6]B. Ferguson and X. C. Zhang, Nat. Mater **1**, 26–33 (2002).
[7]X. C. Zhang, Nature Photon. **4**, 662–662 (2010).
[8]M. B. Johnston, Nature Photon. **1**, 14–15 (2007).
[9]B. T. Hallam *et al.*, Appl. Phys. Lett. **94**, 849 (2004).
[10]S. L. Campanelli, G. Cardano, R. Giannoccaro, A. D. Ludovico, and E. L. J. Bohez, Comput.-Aided Des. **39**, 80–86 (2007).
[11]P. Timbie, J. Grade, D. van der Weide, B. Maffei, and G. Pisano, in *36th International Conference on Infrared Millimeter and Terahertz Waves (IRMMW-THz)* (2011).
[12]S.-H. Park, D-Y. Yang, and K-S. Lee, Laser Photonics Rev. **3**(1–2), 1–11 (2009).
[13]G. O. Mallory and J. B. Hajdu, *Electroless Plating: Fundamentals and Applications* (American Electroplaters and Surface Finishers Society, Orlando, FL, 1990).
[14]F. Felici, T. Goodman, O. Sauter, T. Shimozuma, S. Ito, Y. Mizuno, S. Kubo, and T. Mutoh, Rev. Sci. Instrum. **80**, 013504 (2009).
[15]Y. L. Kok and N. C. Gallagher, J. Opt. Soc. Am. A **5**, 65–73 (1988).
[16]S. K. Jawla, J-Ph. Hogge, and S. Alberti, IEEE Trans. Plasma Sci. **37**, 403–412 (2009).
[17]C. Del Rio Bocio, R. Gonzalo, M. S. Ayza, and M. Thumm, IEEE Trans. Antennas Propag. **47**, 1440–1448 (1999).
[18]E. de Rijk, A. Macor, J-Ph. Hogge, S. Alberti, and J-Ph. Ansermet, Rev. Sci. Instrum. **82**, 066102 (2011).